Inorganic Materials, Vol. 40, No. 12, 2004, pp. 1324–1330. Translated from Neorganicheskie Materialy, Vol. 40, No. 12, 2004, pp. 1508–1514.

Structural and Dielectric Properties of Solid Solutions of Sodium Niobate in Lanthanum and Neodymium Niobates

D. O. Mishchuk, O. I. V'yunov, O. V. Ovchar, and A. G. Belous

Vernadsky Institute of General and Inorganic Chemistry, National Academy of Sciences of Ukraine, pr. Akademika Palladina 32/34, Kiev, 03680 Ukraine

e-mail: belous@ionc.kar.net

Received April 15, 2004

Abstract—Experimental evidence is presented for the formation of continuous series of $Ln_{2/3-x}Na_{3x}\square_{4/3-2x}Nb_2O_6$ (Ln = La, Nd) perovskite-like solid solutions. Increasing the Na content of the solid solutions reduces their symmetry from *Pmmm* to *Pmmn* and then to *Pbcm*. The structural and dielectric properties of the solid solutions belonging to the three space groups are studied.

INTRODUCTION

$NaNbO_3$-based mixed oxides are of considerable interest in designing new functional materials for electronic applications [1, 2]. Partial substitution of La or Nd for Na yields $Ln_{2/3-x}Na_{3x}\square_{4/3-2x}Nb_2O_6$ solid solutions (Ln = La, Nd; □ = vacancy) [3, 4].

Polycrystalline materials prepared on the basis of these solid solutions have recently been found to possess high dielectric permittivity ($\varepsilon \simeq 500$–1000) and low dielectric losses ($\tan\delta \simeq 10^{-3}$) [5, 6]. With increasing Ln content, the phase transition of the solid solutions shifts to lower temperatures, and the temperature coefficient of their permittivity (TCP) changes sign [5, 6]. Data on the crystal structure of $Ln_{2/3-x}Na_{3x}\square_{4/3-2x}Nb_2O_6$ are, however, not available in the literature. There are only high-temperature (>900°C) crystal-chemical data [3, 4], which cannot be correlated with the electrical properties of the solid solutions.

In this work, we describe the structural properties of $Ln_{2/3-x}Na_{3x}\square_{4/3-2x}Nb_2O_6$ (Ln = La, Nd) solid solutions in relation to the dielectric properties of polycrystalline materials.

EXPERIMENTAL

As starting chemicals, we used extrapure-grade La_2O_3, Nd_2O_3, Nb_2O_5, and Na_2CO_3. After calcination of La_2O_3, Nd_2O_3, and Nb_2O_5 at 850°C and Na_2CO_3 at 200°C, appropriate amounts of the reagents were weighed out on a VLP-200 balance and then mixed and homogenized by grinding in a vibratory mill (agate vessels and chalcedony balls) under acetone. Thermal analysis was carried out in a Q-1000 system. After synthesis at 1100–1200°C, the materials were reground in agate vessels with water, dried, and homogenized. Next, a plasticizer was added, and the powders were pressed into disks, which were then sintered between 1200 and 1300°C.

X-ray diffraction (XRD) measurements were made on a DRON-4-07 powder diffractometer (CuK_α radiation, 40 kV, 20 mA). Structural parameters were refined by the Rietveld profile analysis method. XRD patterns were run in the angular range $2\theta = 10°$–$150°$ in a step-scan mode with a step size $\Delta 2\theta = 0.02°$ and a counting time of 10 s per data point. As external standards, we used SiO_2 (2θ calibration) and Al_2O_3 (NIST SRM1976 intensity standard [7]).

Dielectric permittivity ε and losses $\tan\delta$ were measured at 1 MHz using a Tesla BM560 *Q* meter.

RESULTS AND DISCUSSION

XRD data for polycrystalline $Ln_{2/3-x}Na_{3x}\square_{4/3-2x}Nb_2O_6$ (Ln = La, Nd) samples indicate that the perovskite-like structure of the solid solutions may belong to three different space groups, depending on x (Fig. 1). In the composition range $0 \le x \le 0.24$, the two solid-solution phases have a perovskite-like structure ($Ln_{2/3}\square_{4/3}Nb_2O_6$) belonging to the *Pmmm* space group [8]. In the structure of $Ln_{2/3}\square_{4/3}Nb_2O_6$, the Ln atoms are in cuboctahedral oxygen coordination, and the Nb atoms are in octahedral coordination (Fig. 2). Note that the A-site deficient perovskite solid solutions are characterized by additional ordering associated with the high vacancy concentration, which gives rise to additional reflections at $2\theta \sim 13°$ and 29.5° (Fig. 1). The doubling of *c* is due to the alternation of Ln layers with an occupancy of 2/3 (position 1*a*) and vacancy layers (position 1*c*). As shown by Trunov *et al.* [8] and Blasse and Briel [9], the 1*a* sites are filled at random. Characteristically, the Nb atoms in the structure of $Ln_{2/3}\square_{4/3}Nb_2O_6$ are displaced along the *z* axis from the center position toward vacancy (empty) layers. As a

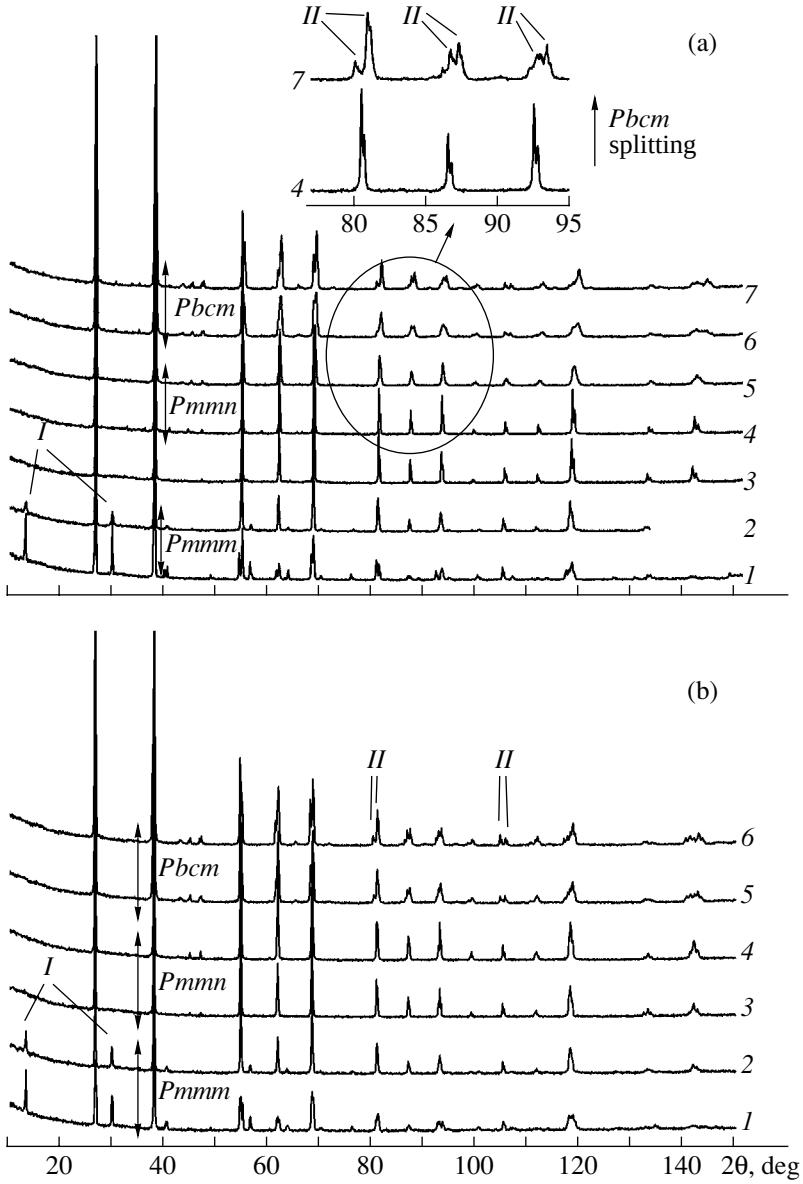

Fig. 1. XRD patterns of polycrystalline $Ln_{2/3-x}Na_{3x}\square_{4/3-2x}Nb_2O_6$ samples: (a) Ln = La, x = (*1*) 0, (*2*) 0.16, (*3*) 0.33, (*4*) 0.39, (*5*) 0.5, (*6*) 0.58, (*7*) 0.66; (b) Ln = Nd, x = (*1*) 0, (*2*) 0.16, (*3*) 0.33, (*4*) 0.5, (*5*) 0.58, (*6*) 0.62. (*I*) reflections corresponding to additional ordering, (*II*) splitting due to the *Pmmn–Pbcm* transition.

result, the Nb–O(1) distance (between Nb atoms and Ln layers) differs from the Nb–O(2) distance (between Nb atoms and vacancy layers).

The dependences of the Nb–O(1) and Nb–O(2) distances on x in the composition range of solid solutions with the $Ln_{2/3}\square_{4/3}Nb_2O_6$ structure ($0 < x \le 0.24$) are displayed in Fig. 3. The Nb displacement along the z axis toward empty cuboctahedra (1*c*) is due to the difference in charge between the planes containing 1*a* and 1*c* sites. Clearly, filling of 1*c* sites with Na ions will increase the charge of the latter plane and reduce that of the plane containing 1*a* sites, leading to Nb displacement toward the center position of the oxygen octahedron. It can be seen in Fig. 3 that, in both the Nd- and La-containing solid solutions, the variations of the Nb–O(1) and Nb–O(2) distances with Na content attest to changes in the charge of crystallographic planes (1*a* and 1*c*). The nature of the lanthanide has no effect on the slope of the lines in Fig. 3.

With increasing x, the space group of the two solid-solution phases changes from *Pmmm* to *Pmmn* (Fig. 1). In the Nd-containing solid solutions, the change in space group is accompanied by little or no change in the volume per formula unit, V/Z (where V is the unit-cell volume), whereas the V/Z of the La-containing solid solutions decreases with increasing x, with a slight break at the *Pmmm–Pmmn* phase boundary (Fig. 4). The observed difference in the variation of V/Z with x

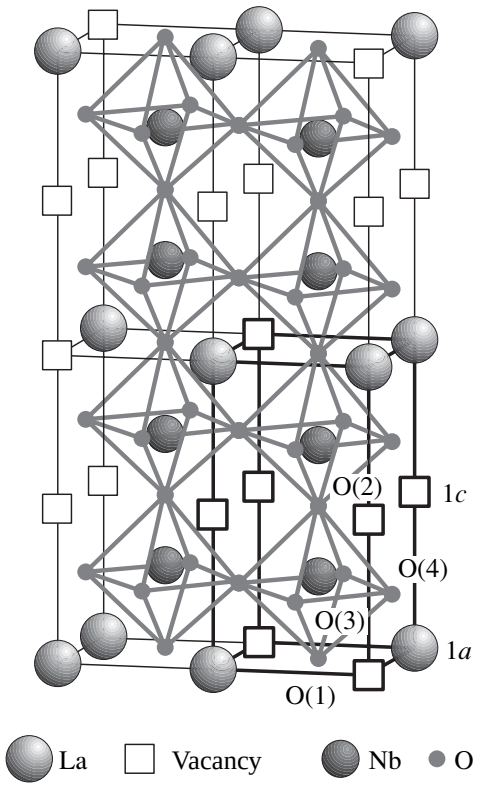

Fig. 2. Structure of the A-site deficient perovskite $La_{2/3}\square_{4/3}Nb_2O_6$ (sp. gr. *Pmmm*): La in position 1*a* (000), Nb in 2*t* (1/2 1/2 *z*), O(1) in 1*f* (1/2 1/2 0), O(2) in 1*h* (1/2 1/2 1/2), O(3) in 2*s* (1/2 0 *z*), O(4) in 2*r* (0 1/2 *z*), and vacancies in 1*c* (0 0 1/2).

is probably associated with the fact that the ionic radius of Na^+ is smaller than that of the host ion La^{3+}, whereas Na^+ and Nd^{3+} are close in ionic radius. Note that, owing to the insignificant difference in ionic radius between Na^+ and Nd^{3+}, the composition range of the *Pmmn* solid solution in the Nd system ($0.24 \le x \le 0.54$) is broader than that in the La system ($0.24 \le x \le 0.45$).

In the ranges $0.54 \le x \le 0.66$ in the Nd system and $0.45 \le x \le 0.66$ in the La system, the space group of the $Ln_{2/3-x}Na_{3x}\square_{4/3-2x}Nb_2O_6$ solid solutions is *Pbcm*, characteristic of $NaNbO_3$ at room temperature [13]. As can be seen in the inset in Fig. 1a, the reduction in the symmetry of $Ln_{2/3-x}Na_{3x}\square_{4/3-2x}Nb_2O_6$ is accompanied by splitting of high-angle reflections. Thus, increasing the Na content of the solid solutions reduces their symmetry from *Pmmm* to *Pmmn* and then to *Pbcm*. Note that the phase transition of antiferroelectric $NaNbO_3$ at 370°C is also accompanied by symmetry reduction from *Pmmn* to *Pbcm* at room temperature [10, 11]. The crystallographic parameters of sodium niobate at room temperature (*P* phase) have not yet been determined. The *P* phase was reported to possess orthorhombic symmetry (sp. gr. no. 57: *Pbma* in a nonstandard setting [12, 13] or *Pbcm* in the standard setting [14]) (Fig. 5). According to Darlington and Knight [15], sodium niobate has a monoclinic structure at room temperature, in line with the expected symmetry reduction by virtue of the ferroelastic constraint upon the $R \xrightarrow{370^\circ C} P$ phase transition. The monoclinic and orthorhombic structures of $NaNbO_3$ are, however, difficult to differentiate even by neutron diffraction [15], and the commonly accepted space group of $NaNbO_3$ is *Pbcm* [13].

The structural parameters of polycrystalline $Ln_{2/3-x}Na_{3x}\square_{4/3-2x}Nb_2O_6$ samples are summarized in Tables 1 and 2. As input data, we took the atomic position coordinates in the structures of $Ln_{2/3-x}\square_{4/3-2x}Nb_2O_6$ [8] and $NaNbO_3$ [13]. Unfortunately, crystallographic data for the *Pmmn* phase of sodium niobate are not available in the literature, and we calculated only the lattice parameters of this phase in our samples.

All of the polycrystalline materials studied in this work offer low microwave losses: $\tan\delta \simeq (1–3) \times 10^{-6}$.

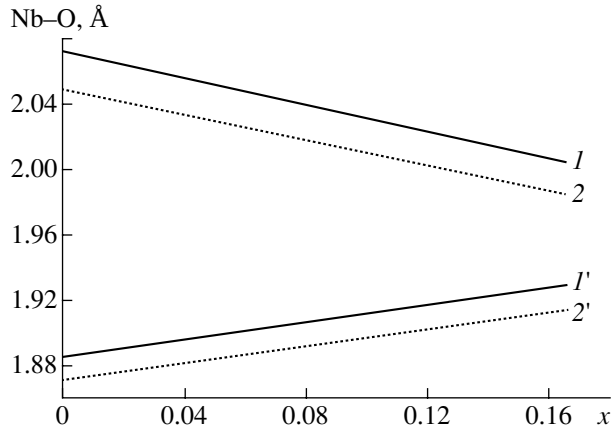

Fig. 3. (*1*, *2*) Nb–O(1) and (*1'*, *2'*) Nb–O(2) distances in the NbO_6 octahedra vs. Na content (*x*) for (*1*, *1'*) $La_{2/3-x}Na_{3x}\square_{4/3-2x}Nb_2O_6$ and (*2*, *2'*) $Nd_{2/3-x}Na_{3x}\square_{4/3-2x}Nb_2O_6$ solid solutions.

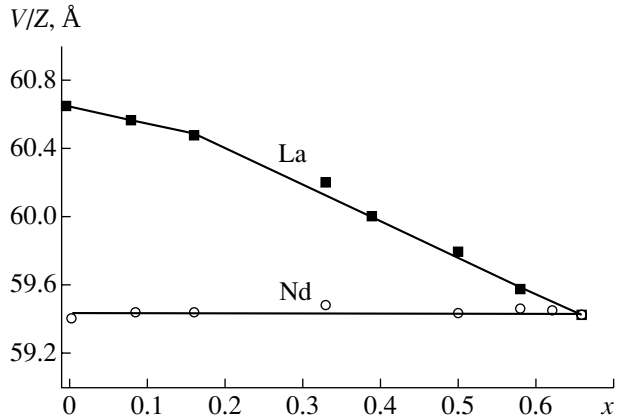

Fig. 4. Composition dependences of the volume per formula unit, *V*/*Z*, for $Ln_{2/3-x}Na_{3x}\square_{4/3-2x}Nb_2O_6$ solid solutions.

Table 1. Crystallographic data for polycrystalline $La_{2/3-x}Na_{3x}\square_{4/3-2x}Nb_2O_6$ samples synthesized at 1350°C

x		0	0.16	0.33	0.39	0.5	0.58	0.66
Sp. gr.		*Pmmm*	*Pmmm*	*Pmmn*	*Pmmn*	*Pbcm*	*Pbcm*	*Pbcm*
a, Å		3.9105(1)	3.921(2)	5.543(7)	5.536(4)	5.5189(3)	5.5100(3)	5.5007(2)
b, Å		3.9197(1)	3.923(2)	7.8389(9)	7.829(1)	5.5458(3)	5.5563(4)	5.5621(2)
c, Å		7.9142(2)	7.8651(7)	5.543(7)	5.536(4)	15.6313(9)	15.5670(9)	15.5373(5)
V, Å^3		121.31(1)	120.97(8)	240.9(4)	240.0(2)	478.43(5)	476.58(5)	475.37(3)
V/Z, Å^3		60.65(1)	60.48(4)	60.2(1)	60.0(1)	59.80(1)	59.57(1)	59.42(1)
La	x	0	0			0.268(9)	0.262(7)	
	y	0	0			0.25	0.25	
	z	0	0			0	0	
Na(1)	x	0	0			0.268(9)	0.262(7)	0.229(5)
	y	0	0			0.25	0.25	0.25
	z	0	0			0	0	0
Na(2)	x					0.25(1)	0.215(6)	0.229(5)
	y					0.225(7)	0.228(6)	0.217(4)
	z					0.25	0.25	0.25
Nb	x	0.5	0.5			0.249(1)	0.254(1)	0.2531(9)
	y	0.5	0.5			0.745(1)	0.741(1)	0.7344(6)
	z	0.2618(2)	0.2547(7)			0.1246(6)	0.1248(5)	0.1251(6)
O(1)	x	0.5	0.5			0.74(2)	0.71(1)	0.678(7)
	y	0.5	0.5			0.25	0.25	0.25
	z	0	0			0	0	0
O(2)	x	0.5	0.5			0.20(1)	0.25(1)	0.213(7)
	y	0.5	0.5			0.813(9)	0.77(1)	0.778(6)
	z	0.5	0.5			0.25	0.25	0.25
O(3)	x	0.5	0.5			0.476(6)	0.468(5)	0.477(4)
	y	0	0			0.461(8)	0.438(4)	0.449(4)
	z	0.267(3)	0.247(9)			0.149(2)	0.158(1)	0.151(1)
O(4)	x	0	0			0.015(7)	0.013(7)	0.035(4)
	y	0.5	0.5			0.009(9)	0.001(6)	0.022(4)
	z	0.223(2)	0.245(9)			0.118(2)	0.117(1)	0.113(2)
Nb–O(1), Å		2.072(2) × 1	2.003(6) × 1			2.01(1) × 1	1.98(1) × 1	1.98(1) × 1
Nb–O(2), Å		1.885(2) × 1	1.929(6) × 1			1.95(1) × 1	1.97(1) × 1	1.97(1) × 1
Nb–O(3), Å		1.960(1) × 2	1.962(2) × 2			2.05(4) × 1	2.12(2) × 1	2.05(2) × 1
						1.97(4) × 1	1.95(3) × 1	1.95(2) × 1
Nb–O(4), Å		1.979(2) × 2	1.962(3) × 2			1.96(4) × 1	1.99(4) × 1	2.01(2) × 1
						1.95(5) × 1	1.97(4) × 1	1.99(2) × 1
⟨Nb–O⟩, Å		1.972(2)	1.963(4)			1.98(3)	1.99(2)	1.99(2)
R_B, %		8.56	9.0			3.76	4.25	3.57
R_f, %		7.36	8.4			5.80	6.09	5.74

Table 2. Crystallographic data for polycrystalline $Nd_{2/3-x}Na_{3x}\square_{4/3-2x}Nb_2O_6$ samples synthesized at 1330°C

x		$x = 0$	$x = 0.16$	$x = 0.33$	$x = 0.5$	$x = 0.58$	$x = 0.62$	$x = 0.66$
Sp. gr		*Pmmm*	*Pmmm*	*Pmmn*	*Pmmn*	*Pbcm*	*Pbcm*	*Pbcm*
a, Å		3.8809(1)	3.8972(2)	5.523(1)	5.522(2)	5.5022(1)	5.5018(1)	5.5007(2)
b, Å		3.9049(2)	3.9086(2)	7.7985(6)	7.7960(6)	5.5532(1)	5.5598(1)	5.5621(2)
c, Å		7.8380(3)	7.8057(6)	5.525(2)	5.522(2)	15.5732(4)	15.5510(3)	15.5373(5)
V, Å^3		118.781(8)	118.90(1)	237.99(9)	237.8(1)	475.83(2)	475.69(2)	475.37(3)
V/Z, Å^3		59.391(4)	59.45(1)	59.49(2)	59.45(2)	59.48(1)	59.46(1)	59.42(1)
La	x	0	0			0.251(6)	0.239(5)	
	y	0	0			0.25	0.25	
	z	0	0			0	0	
Na(1)	x	0	0			0.251(6)	0.239(5)	0.229(5)
	y	0	0			0.25	0.25	0.25
	z	0	0			0	0	0
Na(2)	x					0.226(5)	0.223(4)	0.229(5)
	y					0.222(3)	0.222(3)	0.217(4)
	z					0.25	0.25	0.25
Nb	x	0.5	0.5			0.251(1)	0.2520(7)	0.2531(9)
	y	0.5	0.5			0.7381(5)	0.7359(5)	0.7344(6)
	z	0.2613(3)	0.2548(6)			0.1248(4)	0.1243(3)	0.1251(6)
O(1)	x	0.5	0.5			0.673(6)	0.679(5)	0.678(7)
	y	0.5	0.5			0.25	0.25	0.25
	z	0	0			0	0	0
O(2)	x	0.5	0.5			0.221(8)	0.224(7)	0.213(7)
	y	0.5	0.5			0.767(6)	0.771(5)	0.778(6)
	z	0.5	0.5			0.25	0.25	0.25
O(3)	x	0.5	0			0.466(4)	0.472(3)	0.477(4)
	y	0	0.5			0.446(4)	0.438(3)	0.449(4)
	z	0.244(5)	0.243(3)			0.153(1)	0.1557(9)	0.151(1)
O(4)	x	0	0.5			0.029(4)	0.032(4)	0.035(4)
	y	0.5	0			0.020(4)	0.017(4)	0.022(4)
	z	0.236(5)	0.242(3)			0.117(1)	0.115(1)	0.113(2)
Nb–O(1), Å		2.048(2) × 1	1.989(5) × 1			1.989(9) × 1	1.98(1) × 1	1.98(1) × 1
Nb–O(2), Å		1.871(2) × 1	1.914(5) × 1			1.963(8) × 1	1.971(7) × 1	1.97(1) × 1
Nb–O(3), Å		1.957(3) × 2	1.956(1) × 2			2.05(2) × 1	2.11(2) × 1	2.05(2) × 1
						1.98(2) × 1	1.95(2) × 1	1.95(2) × 1
Nb–O(4), Å		1.951(4) × 2	1.951(1) × 2			1.99(2) × 1	1.99(2) × 1	2.01(2) × 1
						1.96(2) × 1	1.98(2) × 1	1.99(2) × 1
⟨Nb–O⟩, Å		1.956(3)	1.953(2)			1.989(4)	1.99(2)	1.99(2)
R_B, %		8.56	9.0			7.16	6.74	3.57
R_f, %		8.77	9.5			9.5	9.9	5.74

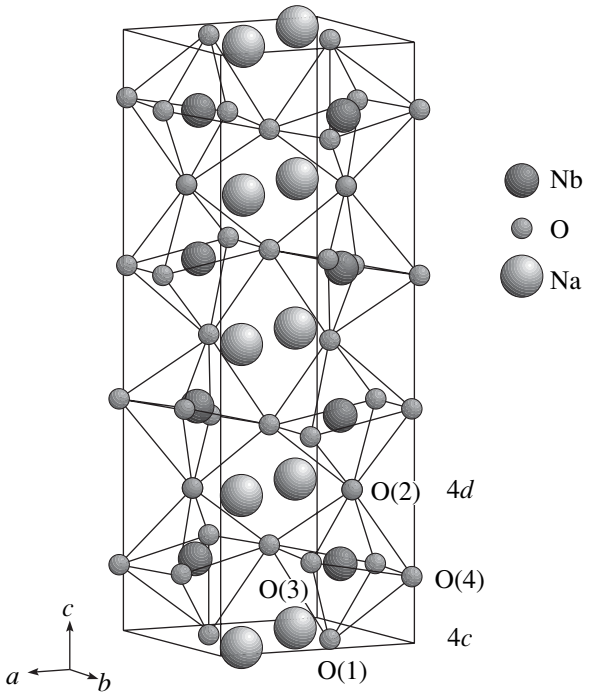

Fig. 5. Perovskite-like structure of $NaNbO_3$ at room temperature (sp. gr. *Pbcm*, no. 57): Na(1) in position 4*c* (*x* 1/4 0), Na(2) in 4*d* (*x y* 1/4), Nb in 8*c* (*xyz*), O(1) in 4*c* (*x* 1/4 0), O(2) in 4*d* (*x y* 1/4), O(3) and O(4) in 8*c* (*xyz*).

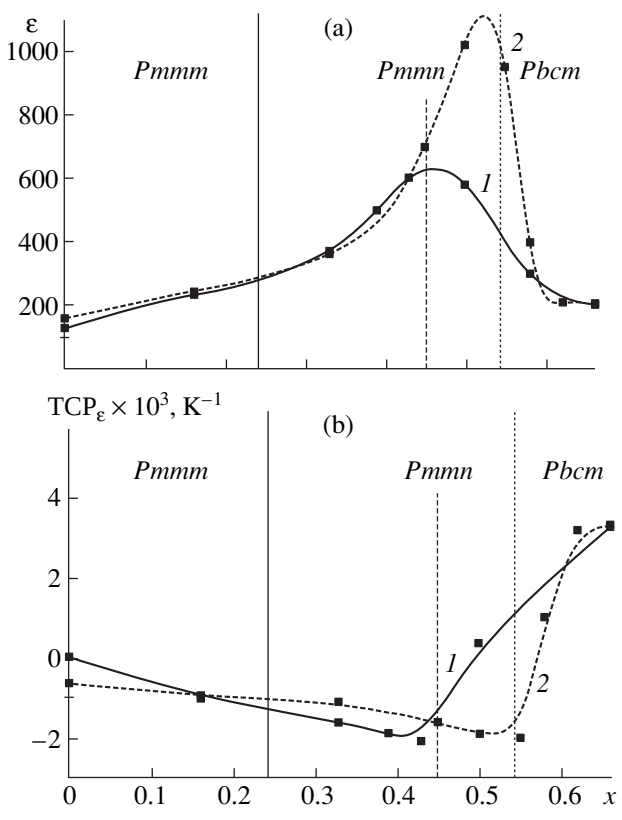

Fig. 6. (a) Dielectric permittivity and (b) TCP vs. Na content for (*1*) $La_{2/3-x}Na_{3x}\square_{4/3-2x}Nb_2O_6$ and (*2*) $Nd_{2/3-x}Na_{3x}\square_{4/3-2x}Nb_2O_6$ solid solutions.

The composition dependences of their dielectric properties are shown in Fig. 6. The permittivity of the solid solutions is seen to be a nonmonotonic function of *x*. In the range $0 \le x \le 0.24$ (*Pmmm* phase), increasing the Na content increases ε only slightly in both the La and Nd systems (Fig. 6a). The likely explanation is that the vacancy layers, containing the 1*c* sites (Fig. 2), restrict the displacement of Nb atoms under the effect of the electric field. The slight increase in ε is due to the reduction in the concentration of cation vacancies. The ε of the *Pmmn* phase is a stronger function of Na content because there is no additional cation ordering. At the *Pmmn–Pbcm* phase boundary, ε passes through a maximum. In the Nd system, this phase boundary lies at a higher Na content and, accordingly, ε_{max} is higher compared to the La system (Fig. 6a).

The change in space group from *Pmmn* to *Pbcm* is also accompanied by a change in the sign of TCP (Fig. 6b). Note that, while negative, the TCP of the La-containing solid solutions varies more rapidly, which can be accounted for by the larger difference in ionic radius between Na^+ and La^{3+}. The present results suggest that the phase transition may broaden and shift to about room temperature.

CONCLUSIONS

We revealed the formation of continuous series of $Ln_{2/3-x}Na_{3x}\square_{4/3-2x}Nb_2O_6$ (Ln = La, Nd) perovskite-like solid solutions which have different space groups, depending on the Na content: *Pmmm* in the range $0 < x \le 0.24$ in the two systems, *Pmmn* in the range $0.24 \le x \le 0.45$ for La and $0.24 \le x \le 0.54$ for Nd, and *Pbcm* in the range $0.45 \le x \le 0.66$ for La and $0.54 \le x \le 0.66$ for Nd. The materials with $0 \le x \le 0.24$ undergo ordering associated with the presence of vacancy layers. In the structure of $Ln_{2/3}\square_{4/3}Nb_2O_6$, the Nb atoms are displaced from the center position in the oxygen octahedra toward the vacancy layers (position 1*c*). Partial Na substitution for La or Nd in the *Pmmm* phase leads to Nb displacement toward the center position of the oxygen octahedra, which is attributable to changes in the charge of crystallographic planes (positions 1*a* and 1*c*). The polycrystalline $Ln_{2/3-x}Na_{3x}\square_{4/3-2x}Nb_2O_6$ materials studied in this work exhibit low microwave losses, $\tan\delta \simeq (2–7) \times 10^{-3}$, and nonmonotonic variations of ε and $\tan\delta$ with Na content. With increasing cation-vacancy concentration, the phase transition of the solid solutions broadens and shifts to lower temperatures. This offers the possibility of preparing materials with a high (300–1000), temperature-stable permittivity.

REFERENCES

1. Reznichenko, L.A., Dergunova, N.V., Geguzina, G.A., *et al.,* $NaNbO_3$-Based Binary Solid Solutions, *Neorg. Mater.*, 1997, vol. 33, no. 12, pp. 1503–1511 [*Inorg. Mater.* (Engl. Transl.), vol. 33, no. 12, pp. 1277–1284].

2. Reznichenko, L.A., Dergunova, N.V., Razumovskaya, O.N., and Shilkina, L.A., Physical Properties of $NaNbO_3$–$A^{2+}TiO_3$ and $NaNbO_3$–$A^{2+}Nb_2O_6$ Solid Solutions, *Neorg. Mater.*, 2001, vol. 37, no. 12, pp. 1525–1534 [*Inorg. Mater.* (Engl. Transl.), vol. 37, no. 12, pp. 1302–1311].
3. Pivovarova, A.P., Strakhov, V.I., and Mel'nikova, O.V., High-Temperature Phase Relations in the $NaNbO_3$–$LaNb_3O_9$ System, *Neorg. Mater.*, 1999, vol. 35, no. 9, pp. 1118–1119 [*Inorg. Mater.* (Engl. Transl.), vol. 35, no. 9, pp. 950–951].
4. Fedorov, N.F., Mel'nikova, O.V., Pivovarova, A.P., and Morozova, E.V., High-Temperature Phase Equilibria in the $NaNbO_3$–$NdNb_3O_9$ System, *Zh. Neorg. Khim.*, 1979, vol. 12, pp. 3350–3353.
5. Mishchuk, D.O., Ovchar, O.V., and Belous, A.G., Chemical Transformations during Synthesis of $(1 - 3x/2)La_{2/3}Nb_2O_6 - 3xNaNbO_3$ Materials and Their Dielectric Properties, *Ukr. Khim. Zh.* (Russ. Ed.), 2002, vol. 68, no. 9, pp. 10–16.
6. Mishchuk, D.O., Ovchar, O.V., and Belous, A.G., Chemical Transformations during Synthesis of $(1 - 3x/2)Nd_{2/3}Nb_2O_6 - 3xNaNbO_3$ Materials and Their Dielectric Properties, *Ukr. Khim. Zh.* (Russ. Ed.), 2003, vol. 69, no. 3, pp. 23–25.
7. *Certificate of Analysis: Standard Reference Material 1976, Instrument Sensitivity Standard for X-ray Powder Diffraction*, Gaithersburg: National Inst. of Standards and Technology, 1991, p. 4.
8. Trunov, V.K., Evdokimov, A.A., Frolov, A.M., and Averina, I.M., Structure Refinement of $La_{0.33}NbO_3$, *Kristallografiya*, 1981, vol. 26, pp. 189–191.
9. Blasse, G. and Briel, A., The Influence of Crystal Structure on the Fluorescence of Oxidic Niobates and Related Compounds, *Z. Phys. Chem. Neue Folge*, 1968, vol. 57, pp. 187–202.
10. Konieczny, K., Dielectric Relaxation in $NaNbO_3$ Single Crystal, *Condens. Matter Phys.*, 1999, vol. 2, no. 4 (20), pp. 655–660.
11. Megaw, H.D., The Thermal Expansion of Interatomic Bonds, Illustrated by Experimental Evidence from Certain Niobates, *Acta Crystallogr., Sect. A: Cryst. Phys., Diffr., Theor. Gen. Crystallogr.*, 1968, vol. 24, pp. 598–604.
12. Ishida, K. and Honjo, G., Soft Modes and Superlattice Structures in $NaNbO_3$, *J. Phys. Soc. Jpn.*, 1973, vol. 34, no. 5, pp. 1279–1288.
13. Sakowski-Cowley, A.C., Lukasszewich, K., and Megaw, H.D., The Structure of Sodium Niobate at Room Temperature, and the Problem of Reliability in Pseudosymmetric Structure, *Acta Crystallogr., Sect. B: Struct. Crystallogr. Cryst. Chem.*, 1969, vol. 25, pp. 851–865.
14. Molak, A. and Kubacki, J., Structure of $NaNbO_3$:*x*Mn Single Crystal at Room Temperature, *Cryst. Res. Technol.*, 2001, vol. 36, pp. 893–902.
15. Darlington, C.N.W. and Knight, K.S., On the Lattice Parameters of Sodium Niobate at Room Temperature and Above, *Physica B* (Amsterdam), 1999, vol. 266, pp. 368–372.